NIH Public Access
Author Manuscript
Ultrasound Med Biol. Author manuscript; available in PMC 2013 November 11.

Published in final edited form as:
Ultrasound Med Biol. 2012 January ; 38(1): . doi:10.1016/j.ultrasmedbio.2011.10.001.

A pilot study to assess markers of renal damage in the rodent kidney after exposure to 7 MHz ultrasound pulse sequences designed to cause microbubble translation and disruption

Kennita Johnson, PhD[1], **Rachel Cianciolo, DVM, DACVP**[2], **Ryan C. Gessner, BS**[1], and **Paul A. Dayton, PhD**[1]

[1]Joint Dept. of Biomedical Engineering, University of North Carolina - North Carolina State University, Chapel Hill, NC, USA

[2]Department of Population Health and Pathobiology, North Carolina State University, Raleigh, NC, USA

Abstract

Acoustic radiation force has been proposed as a mechanism to enhance microbubble concentration for therapeutic and molecular imaging applications. It is hypothesized that once microbubbles are localized, bursting them with acoustic pressure could result in local drug delivery. It is known that low-frequency, high-amplitude acoustic energy combined with cavitation nuclei can result in bioeffects. However, little is known about the bioeffects potential of acoustic parameters involved in radiation-force and microbubble destruction pulse sequences applied at higher frequencies. In this pilot study, rat kidneys are exposed to high-duty cycle, low-amplitude pulse sequences known to cause substantial bubble translation due to radiation force, as well as high-amplitude short pulse sequences known to cause microbubble destruction. Both studies are performed at 7 MHz on a clinical ultrasound system, and implemented in 3-D for entire kidney exposure. Analysis of biomarkers of renal injury and renal histopathology indicate that there was no significant renal damage due to these ultrasound parameters in conjunction with microbubbles within the study group.

Introduction

The combination of microbubbles with ultrasound has contributed to a plethora of both diagnostic and therapeutic applications. Diagnostically, contrast enhanced ultrasound is utilized in echocardiography (Carr and Lindner 2008), determining vessel density (Xiao et al. 2010), estimating tissue blood perfusion (Cosgrove and Lassau 2008; Goldberg et al. 2001; Hoeffel et al. 2010), and in molecular imaging (Gessner and Dayton; 2010). In therapeutic applications acoustically-driven microbubbles have been shown to locally delivery drug and gene payloads (Mayer et al. 2008), enhance vascular permeability (Choi et al. 2010), and increase thermal delivery (Zhang et al. 2011).

When compressible microbubbles interact with a traveling acoustic wave, they experience a radiation force which causes them to translate in the direction of the wave propagation (Dayton et al 1999). A high duty cycle pulse or train of pulses with a low enough pressure so as not to fragment the microbubbles can result in the microbubbles translating tens to hundreds of microns in less than a second (Dayton et al. 2002). Radiation force can readily

Corresponding Author: Paul Dayton, Ph.D. 304 Taylor Hall, CB 7575 Chapel Hill, NC, 27599 Phone: (919) 843 9521 Fax: (919) 843 9520 padayton@bme.unc.edu.

NIH-PA Author Manuscript
NIH-PA Author Manuscript
NIH-PA Author Manuscript

NIH-PA Author Manuscript

NIH-PA Author Manuscript

NIH-PA Author Manuscript

displace microbubbles from the center of a blood vessel to the vascular endothelium in both small and large blood vessels, and thus been proposed as a tool to enhance both molecular imaging as well as targeted drug delivery. In molecular imaging, the use of radiation force to drive targeted microbubbles against the endothelium has been shown to increase the retention of contrast agents at the target site (Zhao et al. 2004; Rychak et al. 2007; Patil et al. 2009). In targeted drug delivery, the ability to displace circulating microbubbles loaded with a therapeutic payload from the blood stream and concentrate them at a site selected by the application of radiation force has been proposed as a way to improve pharmaceutical delivery (Shortencarier et al. 2004; Lum et al. 2006). Radiation force would first be used to concentrate drug-carrying microbubbles, and then high-intensity ultrasound pulses would be utilized to release the drug and perhaps modulate vascular permeability, resulting in increased concentration of the drug in the diseased tissue minimizing the side effects in healthy tissue (Lum et al. 2006; Shortencarier et al. 2004). It is important to note that for both of these applications, the goal is translation of intact microbubbles. Thus, very low acoustic pressures are utilized for microbubble translation, below the threshold of microbubble fragmentation. To achieve substantial displacement at low acoustic pressures, a large duty cycle must be utilized.

The mechanism for bioeffects with ultrasound contrast agents differ from the pharmacological side effects associated with contrast agents for radiographs or magnetic resonance imaging (Williams et al. 2007). The interaction of microbubble contrast agents and ultrasound have the potential to cause bioeffects due to ultrasonic cavitation (Miller et al. 2008). At low ultrasonic pressures, microbubbles undergo sustainable, periodic, radial oscillations in the sound field, termed “stable cavitation” (Flynn 1964). At higher acoustic pressures, the microbubbles can grow and collapse rapidly, often to such a large extent that the microbubbles rupture. This violent collapse can produce substantial shock waves, microjets, microstreaming and free radical formation (Wible et al. 2002; Szabo 2004; Miller et al. 2007; Miller et al. 2008). Previously, the majority of in-vivo studies investigating bioeffects caused by the combination of ultrasound and microbubble contrast agents focused on low-frequency, high-amplitude acoustic energy. Williams et al. (2007) exposed rat kidneys at 1.5 MHz and found that although the visible markings on the kidney surface had faded after 24 hours, there was still evidence of thrombus-like clots in the glomeruli via histology and blood in the urine. Miller et al. (2009) found that some level of the injury persists in the form of fibrosis and scarring in the rat kidney, 1-4 weeks after exposure to 1.5 MHz ultrasound. Miller et al. (2008b) produced glomerular capillary hemorrhage in rat kidneys exposed to ultrasonic frequencies of less than 5 MHz with rarefactional pressure amplitudes between 1.9 and 3.9 MPa. The diagnostic ultrasound system used in the Miller et al. (2008b) study did not produce glomerular capillary hemorrhage at 5 or 7.5 MHz. Wible et al. (2002) discovered that intermittent insonification at frequencies below 5 MHz produces a greater degree of hemorrhage than continuous imaging techniques. Recently, Caskey et al. (2009) have demonstrated that microbubbles insonified with high-duty cycle pulse sequences which cause substantial microbubble translation due to radiation force can cause the formation of holes and tunnels in gelatin phantoms.

To date, there has been no investigation into potential bioeffects caused by radiation force pulse sequences designed to cause substantial microbubble translation without microbubble destruction. Furthermore, there have been few studies investigating the bioeffects of ultrasound and microbubbles at frequencies as high as 7 MHz. Thus, in this pilot study, we investigate the potential of bioeffects for 7 MHz ultrasound in conjunction with microbubbles under conditions intended to first concentrate microbubbles by radiation force, and then disrupt them (as would be implemented in proposed drug-delivery applications). The first condition is a high duty cycle (> 30 %), low amplitude (< 30 kPa) pulse sequence known to cause substantial microbubble translation without destruction (Dayton et al. 2002).

NIH-PA Author Manuscript

NIH-PA Author Manuscript

NIH-PA Author Manuscript

The second condition is a low duty cycle (< 0.1 %), high amplitude (> 5 MPa) pulse sequence, known to cause microbubble destruction (Chomas et al. 2001). Our target organ is the kidney, which is particularly sensitive to bioeffects due to the relatively high blood pressure in the capillary of the glomerulus (Deelman et al. 2010). The potential for glomerular capillary hemorrhage makes the kidney a common model system for evaluating bioeffects from gas body infusion and ultrasound (Miller et al. 2010).

Methods

Animal Preparation

The University of North Carolina Chapel Hill Animal Care and Use Committee approved all experimental procedures. Two cohorts of male Sprague-Dawley rats (N1 = 8, 420g – 535g; N2 = 8, 435g – 501g) were imaged in consecutive identical studies of eight rats each. From each cage, one rat was randomly assigned to receive microbubble destruction pulse sequences and the other rat received radiation force. The animals were anesthetized with 2-3% isoflurane (Halocarbon Laboratories - River Edge, NJ) in a continuous oxygen flow maintained via a nose cone. A 24-gauge indwelling tail vein catheter was inserted to administer microbubble contrast agent. The left flank over the kidney was shaved and a depilatory cream was applied to remove hair. Ultrasound gel was applied to the skin in order to couple the ultrasound transducer to the animal.

Microbubble Destruction

The microbubble contrast agent was a preclinical lipid-shelled, perfluorocarbon microbubble prepared in-house as previously described by (Streeter et al. 2010). The microbubble contrast agent was diluted in saline to get an average concentration of 5.4×10^8 bubbles/ml with a mean diameter of 0.8 (±0.4 SD) μm. Microbubbles were infused through the tail vein catheter via a computer-controlled syringe pump (Harvard Apparatus - Holliston, MA) at 66 μl/min. All ultrasound treatment was performed with an Acuson Sequoia 512 system (Siemens Medical Solutions USA, Inc. – Mountain View, CA) using a 15L8 linear array transducer. One animal per cage (N=8) received destruction-reperfusion parametric imaging technique described previously (Pollard et al. 2009), implemented in 3-Ds (Feingold et al. 2010). This pulse sequence involved clearance of the microbubble contrast agent using a high energy 7 MHz ultrasound pulse sequence for one second (mechanical index (MI) = 1.9, spatial peak temporal average intensity (ISPTA) = 102.67 mW/cm^2, peak negative pressure (PNP) of 5.03 MPa, and a duty cycle of 0.02%), followed by low energy imaging (7 MHz, PRF=16 Hz, MI = 0.18, PNP=476 kPa, ISPTA=0.65 mW/cm^2) in cadence contrast pulse sequencing mode (Phillips and Gardner 2004) for 20 seconds. The pulse sequence was performed once in each location as the transducer was stepped across the entire left kidney at 1-mm increments using a translational stage. This procedure was repeated 3 times successively for the same kidney. The right kidney received no ultrasound and was used as a control.

Radiation Force

Prior to administration of radiation force in-vivo, an in-vitro optimization of radiation force pulses was performed in a phantom environment. Acoustic pulses were administered by the 15L8 ultrasound transducer on microbubble contrast agents pumped through a vertically-oriented 200 μm microtube (Spectrum Labs, Rancho Dominguez, CA) in a waterbath. The effects of these pulses were visualized with a microscope (IX71 - Olympus, Melville, NY) connected to a high speed camera (Photron USA, Inc., Model APX-RS – San Diego, CA). Our radiation force pulse parameters were optimized to maximize microbubble contrast agent translational velocity within the tube. To achieve this, the ultrasound system was set in pulsed wave Doppler mode. The most efficient radiation force was achieved with pulse

NIH-PA Author Manuscript

NIH-PA Author Manuscript

NIH-PA Author Manuscript

amplitudes of 29.7 kPa at a 33% duty cycle and a pulse repetition frequency (PRF) of 17 kHz. Pressures measured were the maximum rarefactional pressure in the beam as determined utilizing a raster scanned needle hydrophone (HNA-0400, ONDA - Sunnyvale, CA) in a water tank. The ISPTA of the pulse was 14.98 mW/cm^2, and the MI was 0.02. Prior to radiation force administration in-vivo, a b-mode image was taken of the left kidney without microbubble contrast agents. One animal per cage (N=8) received radiation force pulse sequences across the left kidney. Microbubble contrast agents was prepared in a similar manner as with microbubble destruction and infused through the tail vein with a syringe pump at 66 μl/min. The radiation force pulse sequences were stepped across the left kidney at 1 mm step sizes with a 20 seconds delay at each step. This was repeated 3 times across the left kidney, thus each location had 1 minute of radiation force pulse administration. The right kidney received no ultrasound and was used as a control.

Urinalysis

Urine was collected from 8 animals (N= 4 from each treatment group) approximately 4 hours after the ultrasound sequence. Urine from all 16 rats was also collected 24 hrs after imaging, prior to euthanasia. Urine dipsticks (Chemstrip 10 with specific gravity, Roche Diagnostics; Indianapolis, IN) were used as a semi-quantitative test for urinary protein to assess acute glomerular injury. Any score above 2+ protein was considered abnormal (Zheng et al. 2005). This test also detects hematuria as red blood cells in the urine causes a strong positive reaction of the urine chemstrip.

Histology

After humanely sacrificing the rats, the left and right kidneys were removed, weighed, and processed for routinely for histology. The remaining organs were examined for gross abnormalities. Specifically, tissues were sectioned at 5 μm and were stained with hematoxylin and eosin. All slides were evaluated by a board certified veterinary pathologist who was blinded to treatment.

Results

The results from the clinical are summarized in Table 1. At necropsy, there were no gross abnormalities in any organs, including the kidneys. Kidney weights were not significantly different between the treatments and their respective controls ($p = 0.09$). For both methods, urinary protein levels were in the trace to 1+ range, which is within normal limits. Figure 1 depicts representative glomeruli and adjacent cortical tubulointerstitium of control (Figure 1A) and imaged (Figure 1B) kidneys from a rat exposed to microbubble destruction. Rats exposed to radiation force had a similar histologic appearance (data not shown). Glomeruli from both treatment groups were normal, as were glomeruli in the contralateral (control) kidneys. There was no evidence of glomerular capillary hemorrhage. Minimal to mild scattered foci of tubular basophilia and atrophy with associated interstitial nephritis were present to similar degrees in both treatment groups and in control kidneys. When present, these rare foci were always <1% of the renal cortex. Because these are chronic, non-specific background lesions commonly observed in normal male rats, they are unrelated to the ultrasonographic treatments. Importantly, neither acute tubular degeneration nor necrosis were present in any animal.

Discussion

In this experiment, rat kidneys were exposed to either “radiation force” or “microbubble destruction” ultrasonic pulse sequences at 7 MHz using a clinical ultrasound system. There were no acute clinical, gross or histologic bioeffects observed which were significant

NIH-PA Author Manuscript

NIH-PA Author Manuscript

NIH-PA Author Manuscript

between control and treated kidneys. A previous study performed at low frequencies had trouble ascertaining the exact location of the scan plane 1-4 weeks after exposures since the markings on the kidney had faded (Miller et al. 2009). This presented a problem for matching histological sections to the kidney exposed to ultrasound. In this study, a 3-D imaging protocol was used to cover the entire kidney for both microbubble destruction and radiation force pulse sequences. This greatly increased our sensitivity to any bioeffects that might have been present since we did not have the challenge of correlating histology with a limited ultrasound treatment area.

The lack of clinical proteinuria at both the 4- and 24-hours time points indicates that the glomerular basement membrane remained intact and functional and that the proximal tubule was retained its capacity to reabsorb filtered proteins. Although minimal to mild renal lesions were observed histologically, both treatment groups were similarly affected and inflammation was present in the treated kidneys to a similar degree as control kidneys. The tubular and interstitial lesions present in these animals are common background renal lesions in adult male Sprague-Dawley rats. Their chronicity and association with similar lesions in the kidneys not exposed to ultrasound suggest that the lesions were pre-existing and not associated with treatment.

To date, there have been no published bioeffects analyses based on pulse sequences designed to cause microbubble translation without destruction. Although Caskey et al. (2009) observed substantial pore formation and tunnel boring due to radiation force mediated microbubble translation in gel phantoms, the acoustic pressures utilized here (<50 kPa) were much lower than those evaluated by Caskey (>600 kPa). Additionally, the effects observed by Caskey were most significant at lower frequencies (1 and 2.25 MHz), and minimal at 5 MHz. They did not perform studies as high as 7 MHz, as was studied here. It is important to note also that Caskey observed substantial differences in pore formation in gelatin due to microbubbles as a function of microbubble concentration, which was a variable that we did not evaluate.

Observations in this study of microbubble destruction pulses agree with previous studies seen in the literature. Wible et al. (2002) found that rat kidneys exposed to higher frequency (> 5 MHz), low output power ultrasound caused minimal biological alterations. Increases in the imaging frequency reduced the intensity and amount of change to the renal surface during intermittent insonification (Wible et al. 2002). During continuous ultrasound exposure at the higher frequencies (4 and 6 MHz), there was little to no hemorrhage on the renal surface (Wible et al. 2002). Miller et al. (2008b) found that for the highest frequencies (5 and 7.5 MHz), the kidney did not yield any significant glomerular capillary hemorrhage by either visual inspection or histology.

Conclusion

This pilot study presents initial data concerning the safety of acoustic radiation force pulse sequences which cause substantial microbubble translation without destruction, as well as microbubble-destruction pulse sequences at 7 MHz. As more targeted imaging or therapeutics strategies are implemented, it is important to know the potential of hazards to surrounding tissue that would be produced by the use of microbubbles and ultrasound. Although this study was substantially limited by its small size and limited parameter ranges, our initial findings of the lack of bioeffects are encouraging.

Acknowledgments

The authors appreciate the assistance of Ismayil Guracar, from Siemens Medical Solutions, in determination of the exposure parameters from the Sequoia imaging system. P.A.D. is on the Scientific Advsory Board for Targeson Inc.

NIH-PA Author Manuscript

NIH-PA Author Manuscript

NIH-PA Author Manuscript

The Dayton Lab has collaborations with Siemens Medical Solutions, Visualsonics, Inc., and Lantheus Medical Imaging, Inc., although none of these collaborations involve financial exchange. Financial support for this work was provided by the NIH through grant R01EB008733-01A1.

References

Carr CL, Lindner JR. Myocardial perfusion imaging with contrast echocardiography. Curr Cardiol Rep. 2008; 10:233–9. [PubMed: 18489868]

Caskey CF, Qin S, Dayton PA, Ferrara KW. Microbubble tunneling in gel phantoms. J Acoust Soc Am. 2009; 125:EL183–9. [PubMed: 19425620]

Choi JJ, Wang S, Tung YS, Morrison B 3rd, Konofagou EE. Molecules of various pharmacologically-relevant sizes can cross the ultrasound-induced blood-brain barrier opening in vivo. Ultrasound Med Biol. 2010; 36:58–67. [PubMed: 19900750]

Chomas JE, Dayton P, May D, Ferrara K. Threshold of fragmentation for ultrasonic contrast agents. J Biomed Opt. 2001; 6:141–50. [PubMed: 11375723]

Cosgrove D, Lassau N. Imaging of perfusion using ultrasound. Eur J Nucl Med Mol Imaging. 2008; 37(Suppl 1):S65–85. [PubMed: 20640418]

Dayton PA, Allen JS, Ferrara KW. The magnitude of radiation force on ultrasound contrast agents. J Acoust Soc Am. Nov.2002 112:2183–92. [PubMed: 12430830]

Dayton PA, Morgan KE, Klibanov AL, Brandenburger GH, Ferrara KW. Optical and acoustical observations of the effects of ultrasound on contrast agents. IEEE Trans Ultrason Ferroelectr Freq Control. 1999; 46:220–32. [PubMed: 18238417]

Deelman LE, Declèves A-E, Rychak JJ, Sharma K. Targeted renal therapies through microbubbles and ultrasound. Advanced Drug Delivery Reviews. 2010; 62:1369–77. [PubMed: 20946925]

Feingold S, Gessner R, Guracar IM, Dayton PA. Quantitative volumetric perfusion mapping of the microvasculature using contrast ultrasound. Invest Radiol. 2010; 45:669–74. [PubMed: 20808232]

Flynn, HG. Physics of acoustic cavitation in liquids. In: Mason, WP., editor. Physical Acoustics, Principles and Methods 1B. Academic Press; New York, NY: 1964. p. 57-172.

Gessner R, Dayton PA. Advances in molecular imaging with ultrasound. Mol Imaging. 2010; 9:117–27. [PubMed: 20487678]

Goldberg, B.; Raichlen, J.; Forsberg, F. Ultrasound Contrast Agents: Basic Prinicples and Clinical Applications. 2nd edition. Martin Dunitz Ltd; London: 2001.

Hoeffel C, Mule S, Huwart L, Frouin F, Jais JP, Helenon O, Correas JM. Renal blood flow quantification in pigs using contrast-enhanced ultrasound: an ex vivo study. Ultraschall Med. 2010; 31:363–9. [PubMed: 20408121]

Lum AF, Borden MA, Dayton PA, Kruse DE, Simon SI, Ferrara KW. Ultrasound radiation force enables targeted deposition of model drug carriers loaded on microbubbles. J Control Release. 2006; 111:128–34. [PubMed: 16380187]

Mayer CR, Geis NA, Katus HA, Bekeredjian R. Ultrasound targeted microbubble destruction for drug and gene delivery. Expert Opin Drug Deliv. 2008; 5:1121–38. [PubMed: 18817517]

Miller DL, Averkiou MA, Brayman AA, Everbach EC, Holland CK, Wible JH Jr. Wu J. Bioeffects considerations for diagnostic ultrasound contrast agents. J Ultrasound Med. 2008a; 27:611–32. quiz 33-6. [PubMed: 18359911]

Miller DL, Dou C, Wiggins RC. Frequency dependence of kidney injury induced by contrast-aided diagnostic ultrasound in rats. Ultrasound Med Biol. 2008b; 34:1678–87. [PubMed: 18485567]

Miller DL, Dou C, Wiggins RC. In vivo gas body efficacy for glomerular capillary hemorrhage induced by diagnostic ultrasound in rats. IEEE Trans Biomed Eng. 2010; 57:167–74. [PubMed: 19709948]

Miller DL, Dou C, Wiggins RC, Wharram BL, Goyal M, Williams AR. An in vivo rat model simulating imaging of human kidney by diagnostic ultrasound with gas-body contrast agent. Ultrasound Med Biol. 2007; 33:129–35. [PubMed: 17189055]

Patil AV, Rychak JJ, Allen JS, Klibanov AL, Hossack JA. Dual frequency method for simultaneous translation and real-time imaging of ultrasound contrast agents within large blood vessels. Ultrasound Med Biol. 2009; 35:2021–30. [PubMed: 19828229]

NIH-PA Author Manuscript

NIH-PA Author Manuscript

NIH-PA Author Manuscript

Phillips P, Gardner E. Contrast-agent detection and quantification. Eur Radiol. 2004; 14(Suppl 8):P4–10. [PubMed: 15700327]

Pollard RE, Dayton PA, Watson KD, Hu XW, Guracar IM, Ferrara KW. Motion Corrected Cadence CPS Ultrasound for Quantifying Response to Vasoactive Drugs in a Rat Kidney Model. Urology. 2009; 74:675–81. [PubMed: 19589583]

Rychak JJ, Klibanov AL, Ley KF, Hossack JA. Enhanced targeting of ultrasound contrast agents using acoustic radiation force. Ultrasound in Medicine and Biology. 2007; 33:1132–9. [PubMed: 17445966]

Shortencarier MJ, Dayton PA, Bloch SH, Schumann PA, Matsunaga TO, Ferrara KW. A method for radiation-force localized drug delivery using gas-filled lipospheres. Ieee Transactions on Ultrasonics Ferroelectrics and Frequency Control. 2004; 51:822–31.

Streeter JE, Gessner R, Miles I, Dayton PA. Improving sensitivity in ultrasound molecular imaging by tailoring contrast agent size distribution: in vivo studies. Mol Imaging. 2010; 9:87–95. [PubMed: 20236606]

Szabo, T. Diagnostic Ultrasound Imaging: Inside Out. Elsevier; Burlington, MA: 2004.

Wible JH Jr. Galen KP, Wojdyla JK, Hughes MS, Klibanov AL, Brandenburger GH. Microbubbles induce renal hemorrhage when exposed to diagnostic ultrasound in anesthetized rats. Ultrasound Med Biol. 2002; 28:1535–46. [PubMed: 12498949]

Williams AR, Wiggins RC, Wharram BL, Goyal M, Dou C, Johnson KJ, Miller DL. Nephron injury induced by diagnostic ultrasound imaging at high mechanical index with gas body contrast agent. Ultrasound Med Biol. 2007; 33:1336–44. [PubMed: 17507144]

Xiao JD, Zhu WH, Shen SR. Evaluation of hepatocellular carcinoma using contrast-enhanced ultrasonography: correlation with microvessel morphology. Hepatobiliary Pancreat Dis Int. 2010; 9:605–10. [PubMed: 21134829]

Zhang M, Fabiilli ML, Haworth KJ, Padilla F, Swanson SD, Kripfgans OD, Carson PL, Fowlkes JB. Acoustic Droplet Vaporization for Enhancement of Thermal Ablation by High Intensity Focused Ultrasound. Acad Radiol. 2011

Zhao S, Borden M, Bloch SH, Kruse D, Ferrara KW, Dayton PA. Radiation-force assisted targeting facilitates ultrasonic molecular imaging. Mol Imaging. 2004; 3:135–48. [PubMed: 15530249]

Zheng Z, Schmidt-Ott KM, Chua S, Foster KA, Frankel RZ, Pavlidis P, Barasch J, D'Agati VD, Gharavi AG. A Mendelian locus on chromosome 16 determines susceptibility to doxorubicin nephropathy in the mouse. Proceedings of the National Academy of Sciences of the United States of America. 2005; 102:2502–7. [PubMed: 15699352]

NIH-PA Author Manuscript
NIH-PA Author Manuscript
NIH-PA Author Manuscript

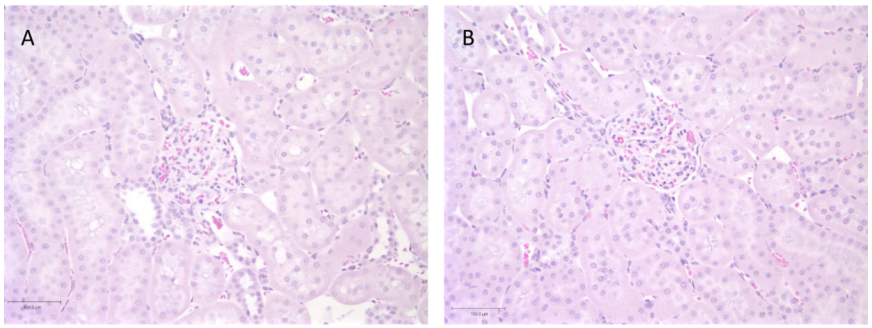

Figure 1.
Photomicrographs of representative glomeruli and tubules of control (A) and imaged (B) kidneys from a rat exposed to microbubble destruction. The glomeruli are normal, tubular necrosis and degeneration are absent, and there is no interstitial inflammation. Of note, the brush borders of proximal tubules are intact in both kidneys. Hematoxylin and eosin, 20X magnification.

NIH-PA Author Manuscript

NIH-PA Author Manuscript

NIH-PA Author Manuscript

Table 1

Clinical parameters of left (imaged) and right (control) kidneys exposed to either MBD or RF via ultrasound.

Rat ID	Treatment	Body Wt in g	Lt Kid. Wt in g (% BW)	Rt Kid. Wt in g (% BW)	Urine Protein Chemstip
504	MBD	547	1.6 (0.3%)	1.6 (0.3%)	Trace
588	MBD	535	1.9 (0.4%)	2.0 (0.4%)	1+
593	MBD	421	1.7 (0.4%)	1.4 (0.3%)	Trace
895	MBD	450	1.7 (0.4%)	1.5 (0.3%)	Trace
524	RF	527	1.5 (0.3%)	1.7 (0.3%)	Trace
525	RF	479	1.8 (0.4%)	2.0 (0.4%)	1+
595	RF	519	1.9 (0.4%)	2.1 (0.4%)	1+
596	RF	491	1.7 (0.3%)	1.6 (0.3%)	1+

NIH-PA Author Manuscript

NIH-PA Author Manuscript

NIH-PA Author Manuscript

Table 2

Histological evaluations of left (imaged) and right (control) kidneys exposed to either microbubble destruction (MBD) or radiation force (RF) via ultrasound.

		Left Kidney			Right Kidney		
Rat ID	**Treatment**	**Glomeruli**	**Tubules**	**Interstitium**	**Glomeruli**	**Tubules**	**Interstitium**
504	MBD	Normal	Normal	Normal	Normal	Normal	Normal
588	MBD	Normal	Normal	Normal	Normal	#	*
593	MBD	Normal	Normal	***	Normal	#	***
895	MBD	Normal	Normal	Normal	Normal	Normal	Normal
524	RF	Normal	Normal	Normal	Normal	Normal	Normal
525	RF	Normal	#	*	Normal	Normal	Normal
595	RF	Normal	#	*	Normal	Normal	Normal
596	RF	Normal	Normal	**	Normal	Normal	**

*Minimal chronic inflammation associated with tubular lesion;

**Minimal multifocal chronic inflammation;

***Mild multifocal chronic inflammation;

#Focal tubular basophilia with protein casts